Divergent evapotranspiration partition dynamics between shrubs and grasses in a shrub-encroached steppe ecosystem

Article *in* New Phytologist · June 2018

DOI: 10.1111/nph.15237

CITATIONS
0

READS
314

7 authors, including:

Pei Wang
Beijing Normal University
24 PUBLICATIONS **139** CITATIONS
SEE PROFILE

Xiao-Yan Li
Beijing Normal University
138 PUBLICATIONS **2,283** CITATIONS
SEE PROFILE

Lixin Wang
Indiana University-Purdue University Indianapolis
178 PUBLICATIONS **2,396** CITATIONS
SEE PROFILE

Xiuchen Wu
Beijing Normal University
61 PUBLICATIONS **459** CITATIONS
SEE PROFILE

New Phytologist

Research

Divergent evapotranspiration partition dynamics between shrubs and grasses in a shrub-encroached steppe ecosystem

Pei Wang[1,2], Xiao-Yan Li[1,2], Lixin Wang[3], Xiuchen Wu[1,2], Xia Hu[1,2], Ying Fan[2] and Yaqin Tong[2]

[1]State Key Laboratory of Earth Surface Processes and Resource Ecology, Beijing Normal University, Beijing 100875, China; [2]School of Natural Resources, Faculty of Geographical Science, Beijing Normal University, Beijing 100875, China; [3]Department of Earth Sciences, Indiana University–Purdue University Indianapolis, Indianapolis, IN 46202, USA

Author for correspondence:
Pei Wang
Tel: *+86 1058800148*
Email: peiwang@bnu.edu.cn

Received: *9 December 2017*
Accepted: *22 April 2018*

New Phytologist (2018)
doi: 10.1111/nph.15237

Key words: canopy resistance, ecohydrological connectivity, evapotranspiration partitioning, numerical modeling, shrub encroachment, two-source mixing, water-use patterns.

Summary

- Previous evapotranspiration (ET) partitioning studies have usually neglected competitions and interactions between antagonistic plant functional types. This study investigated whether shrubs and grasses have divergent ET partition dynamics impacted by different water-use patterns, canopy structures, and physiological properties in a shrub-encroached steppe ecosystem in Inner Mongolia, China.
- The soil water-use patterns of shrubs and grasses have been quantified by an isotopic tracing approach and coupled into an improved multisource energy balance model to partition ET fluxes into soil evaporation, grass transpiration, and shrub transpiration.
- The mean fractional contributions to total ET were $24 \pm 13\%$, $20 \pm 4\%$, and $56 \pm 16\%$ for shrub transpiration, grass transpiration, and soil evaporation respectively during the growing season. Difference in ecohydrological connectivity and leaf development both contributed to divergent transpiration partitioning between shrubs and grasses.
- Shrub-encroachment processes result in larger changes in the ET components than in total ET flux, which could be well explained by changes in canopy resistance, an ecosystem function dominated by the interaction of soil water-use patterns and ecosystem structure. The analyses presented here highlight the crucial effects of vegetation structural changes on the processes of land–atmosphere interaction and climate feedback.

Introduction

Shrub encroachment is emerging as a widespread global phenomenon in arid and semi-arid regions (Van Auken, 2000; D'Odorico *et al.*, 2011; Eldridge *et al.*, 2011; Li *et al.*, 2013), which is reported to be triggered by climate change, grazing, and/or fire management practices (Neilson, 1986; Archer *et al.*, 1995; Coetzee *et al.*, 2008) and has important biogeochemical and ecohydrological consequences (Archer *et al.*, 1995; Huxman *et al.*, 2005; Scott *et al.*, 2006b). Shrub encroachment results in a shift in plant community composition and alters environmental microclimates, creating a positive feedback with plant growth leading to its expansion (He *et al.*, 2010; D'Odorico *et al.*, 2013; Li *et al.*, 2013). Shrub encroachment is generally associated with reductions in ecosystem functioning (Van Auken, 2000, 2009; Archer, 2010). Such changes in plant community composition highlight the influence of vegetation on the hydrological cycle and provide important insights into the biological feedbacks that must be understood to achieve better prediction of terrestrial–atmospheric coupling (Huxman *et al.*, 2005; Jasechko *et al.*, 2013). However, the impact of shrub encroachment on regional climate conditions remains poorly investigated. Evapotranspiration (ET) is a crucial process within the soil–plant–atmosphere continuum (SPAC) and is a major component of the annual water–energy balance. The ET flux in terrestrial ecosystems is a combination of two or three different pathways (e.g. plant transpiration, soil evaporation, and canopy interception) of water vaporization (Wang *et al.*, 2010; Katul *et al.*, 2012). When considering shrub encroachment in ecosystems, it is important to investigate different components of ET to understand the coupling of ecohydrological processes and vegetation functioning, carbon, and climate feedback and to improve the management of water resources (Kool *et al.*, 2014; Fisher *et al.*, 2017). However, these shrub-encroached ecosystems are commonly heterogeneous savanna-like ecosystems, with contrasting plant functional types (PFTs, e.g. grasses and shrubs) competing for the water use. Despite the attention these ecosystems are receiving, a general lack of knowledge persists about the relationship between ET and the plant adaptation strategies for the different PFTs under wet/dry seasons. Indeed, for surviving, the different PFTs need to adapt their rooting systems (in terms of depth and vertical distribution) to the soil moisture content profile, but at the same time the species will compete between themselves with contrasting water-use strategies (Wu *et al.*, 2017).

Ecohydrological connectivity is described as an ecosystem property that represents the water-flow linkages through the SPAC, by which feedbacks and other emergent system behaviors may be generated (Miller *et al.*, 2012; Wang *et al.*, 2012).

Quantifying the role of ecohydrological connectivity is important because if partitioning is tied to ecohydrological connectivity, then accurate predictions of future water availability will require a more detailed understanding of the underlying processes controlling plant–water interactions that are currently included in most hydrological models. Previous studies showed that hydrologic connectivity constrains the partitioning of global terrestrial water fluxes (Good *et al.*, 2015). Considering the connections between surface and subsurface water interaction in model simulations has shown promise for improving ET partitioning accuracy (Maxwell & Condon, 2016). However, ecohydrological connectivity for different PFTs remains to be quantified and incorporated into ET partitioning estimates (Brooks *et al.*, 2015). Shrub-encroached ecosystems have different PFTs (shrubs and grasses), which create high spatial heterogeneity of the canopy structure and have different rooting architectures (Eldridge *et al.*, 2011). With their inherent patchy distributions, shrub-encroached ecosystems are ideal for exploring the biophysical dynamics within the framework of ecohydrological connectivity and studying the property changes of an ecosystem shifting from grass- to shrub-dominated states. In this work, the vertical ecohydrological connections were quantified on several levels for both shrubs and grasses (Fig. 1). The first connection is the upward movement of water through the SPAC (plant transpiration, evaporation from soil) or simply the soil–atmosphere continuum (soil evaporation), which can be generalized by using electrical circuit theory and modeling ET as the resistance terms (e.g. canopy resistance, aerodynamic resistance, and surface soil resistance) (Jones, 1992; Wang *et al.*, 2012). The second connection is upward movement of water from different soil layers through root uptake. The root uptake reflects a plant's survival strategy and controls transpiration fluxes. Despite its importance, there is still no reliable method for reconstructing water-use patterns. Stable isotopes of hydrogen and oxygen provide a promising tool to qualify vegetation water-use patterns and are extensively used in plant–water relation research to investigate physiological and hydrological processes from whole-plant to ecosystem scales (Kendall & McDonnell, 1998; Wang *et al.*, 2015, 2016; Sprenger *et al.*, 2016; Zhao *et al.*, 2016).

Several methods have been used in previous studies to partition ET and to qualify the effects of shrub encroachment on the partitioned ET, including field experiments (e.g. Scott *et al.*, 2006a,b; Moran *et al.*, 2009), isotope methods (Williams *et al.*, 2004; Jasechko *et al.*, 2013), and a water-balance modeling approach (e.g. Huxman *et al.*, 2005). However, these partitioning research studies rely on either isotope approaches or terrestrial biosphere models. These are fundamentally different methods, and both types of methods lack the complex interaction between vegetation and atmosphere that occurs in shrub-encroached ecosystems. How to represent vegetation dynamics adequately in shrub-encroached ecosystems has challenged current approaches (e.g. isotope methods or terrestrial biosphere models) when assessing the mechanisms underlying changes in ET or *T*/ET as a result of shrub encroachment (Huxman *et al.*, 2005; Whitley *et al.*, 2016). To investigate these mechanisms, an approach should be able to adequately represent the biophysical dynamics of

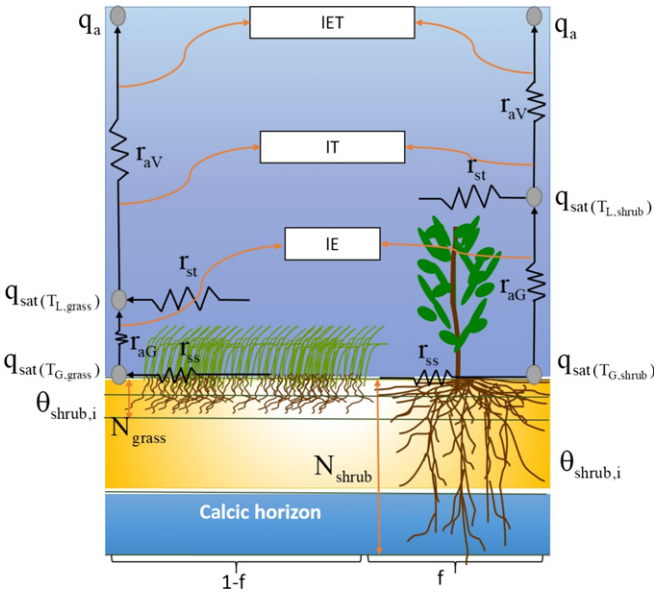

Fig. 1 Schematic illustration of ecohydrological connectivity considered in a shrub-encroached ecosystem. Symbols are defined in Supporting Information Table S4.

shrub-encroached ecosystems. Particular attributes of shrub-encroached ecosystems, such as characteristic traits and behaviors of shrubs and grasses and how these differ across the seasonality of available soil water, must be considered. A two-source model that considers the energy balances of the vegetation canopy and the ground surface separately and also the interaction between them (Shuttleworth & Wallace, 1985; Wang & Yamanaka, 2014) is relatively simple, but can still consider vertical water connections via the SPAC (plant transpiration, evaporation from soil) or just the soil–atmosphere continuum (soil evaporation). These connections can integrate isotopic processes with water exchange in terrestrial ecosystems and have the advantage of tracing plant water-use patterns (Wang *et al.*, 2015; Sprenger *et al.*, 2016). In this study, three dynamic processes that directly affect the biophysical processes of a shrub-encroached ecosystem (root-water access, canopy structure, and physiological properties) have been highlighted. Furthermore, the two-source model is also a useful tool for aggregating different cover types (e.g. shrubs and grasses) in a shrub-encroachment ecosystem to estimate ET and its components (Norman & Becker, 1995; Norman *et al.*, 2003; Anderson *et al.*, 2004; Li *et al.*, 2008; Guan & Wilson, 2009).

The grassland of Inner Mongolia in China, which is representative of the Eurasian steppe region, is an important rangeland that sustains the livelihood of a nomadic population. In the typical steppe ecosystem of the Inner Mongolia grassland, *Caragana microphylla* Lam. (*C. microphylla*) cover has expanded due to the increase in grazing in recent decades (Peng *et al.*, 2013; Li *et al.*, 2013). The efficient use of the limited water resources is essential for sustaining livestock farming, which requires the productive water loss *T* to be maximized and the unproductive water loss *E* to be minimized (Wang & D'Odorico, 2008). There have been many studies on ET in this region (Li *et al.*, 2013; Peng *et al.*,

2013; Zhang *et al.*, 2013); however, owing to the difficulty of partitioning ET into transpiration of different PFTs and soil evaporation, there have been few studies focusing on the effect of shrub encroachment on ET partitioning, and the hydrological implications of shrub encroachment remain rarely investigated in arid and semiarid regions. There is a lack of reliable ET partitioning models and suitable model parameters for shrub-encroachment ecosystems. In this work, the impacts of shrub encroachment on ET and its components were investigated numerically using a two-source surface energy balance model. The objectives of the study were (i) to partition ET flux components in shrub-encroached grassland considering their ecohydrological connectivity, and (ii) to determine the effect of shrub encroachment on ET and its components (*E*/ET or *T*/ET).

Materials and Methods

Study site

The study was conducted at the Farmland and Grassland Ecosystem Observation Station of Beijing Normal University located in Taipus Banner, Inner Mongolia, North China (42°07′59.2″N, 115°26′31.5″E). The mean annual temperature at the site is 1.6°C, the mean annual precipitation is 392 mm, and mean annual pan evaporation is 1900 mm. The active plant growing season in this area ranges from June to August. The dominant grass species is *Stipa krylovii* Roshev. The *C. microphylla* shrub covers 15.0% of the site. It is reported that the area of *C. microphylla* encroaching upon grassland amounts to $>5.1 \times 10^6$ ha (Zhang *et al.*, 2006; Li *et al.*, 2013). Shrub encroachment along a zone of increasing intensity of anthropogenic disturbance in this area was investigated and classified as lightly, moderately, and seriously disturbed grasslands, which were characterized by shrub coverages of 25%, 31.4% and 43.5% respectively (Peng *et al.*, 2013).

Bowen ratio system and field isotopic measurements

Bowen ratio towers (Dynamax Inc., Houston, TX, USA) were set up to measure the meteorological data and estimate ET. Using these data, ET was calculated using the Bowen ratio method. A data logger (CR1000, Campbell Scientific, Logan, UT, USA) was used to record meteorological data at 10 min intervals. Air temperature and relative humidity were recorded with a CS500 temperature and relative humidity probe (Campbell Scientific) at heights of 2.0 and 1.5 m. Precipitation was measured with a tipping bucket rain gauge (Model TE525). A silicon radiation sensor (LI-200SZ, Li-Cor, Lincoln, NE, USA) was used to measure solar radiation, and a net radiometer (SNR01) was used to measure net radiation. Wind speed was recorded by a three-cup anemometer (RM Young Model 03001; RM Young Co., Traverse City, MI, USA) positioned 3 m above the ground. The towers were powered by solar panels. Soil water content was measured by ECH$_2$O 5TE sensors placed under grass and shrub patches and was validated monthly using an oven-drying method. The leaf area index LAI, shrub coverage *f*, and height of shrubs and grasses were measured at monthly intervals during the growing season. The LAI and canopy height Z_V of grasses were estimated as a weighted mean between the measured values in the interspace between shrubs and beneath the shrub canopy. Leaf temperature measurements were made at 09:00–15:00 h China Standard Time for 3 d at monthly intervals throughout the growing season. On each day, leaf temperature T_L was measured 60 times within a 1 h period for randomly selected leaves very close to each other (3–5 cm) by a handheld infrared-radiation thermometer (PT-7LD, Optex, Shiga, Japan). Samples of stem water from both shrubs and grasses and belowground soil water from the 0–10, 10–20, 20–40, 40–60 and 60–100 cm layers were collected at monthly time intervals during the growing season. Stem and soil water samples with three replicates were extracted in the laboratory by cryogenic vacuum distillation (West *et al.*, 2006). The stable hydrogen and oxygen isotope compositions in stem water and soil water were determined by an isotopic ratio infrared spectroscopy system (LWIA, DLT-100; Los Gatos Research Inc., Mountain View, CA, USA) at the State Key Laboratory of Earth Surface Process and Resource Ecology, Beijing Normal University. All laboratory standards were calibrated against international reference materials that determine the Vienna standard mean ocean water–standard light Antarctic precipitation scale provided by the International Atomic Energy Agency. The long-term analytical uncertainty (one standard deviation) was determined as 1‰ for δ^2H and 0.1‰ for $\delta^{18}O$.

Model description

A detailed description of the model is provided in Supporting Information Methods S1 and Fig. S1. Briefly, a two-source model was updated here to simulate the hourly energy (R_n, lET, *H* and *G*) and ET, *E* and *T* fluxes (Wang & Yamanaka, 2014). The model was selected for several reasons. First, this model treats the radiation/energy balance properly both in the aggregated vegetative canopy (Eqn S1-1 in Methods S1) and at the ground surface (Eqn S1-2) with interaction between them. This makes it possible to estimate all the energy balance components (Eqn S4-8), including the latent heat flux lET and its components lE and lT. Second, the interaction between vegetation and the atmosphere that occurs in a shrub-encroached ecosystem can be represented by aggregating the different ecohydrological connectivities between shrubs and grasses. As shown in Fig. 1, the vertical ecohydrological connectivity was quantified at several levels and aggregated between shrubs and grasses by modeling lET as resistance terms (Jones, 1992; Wang *et al.*, 2012) in shrub-encroached ecosystems. Stomatal control of transpiration, including its dependence on soil moisture availability and the nonlinear response of plant physiology to light penetration inside the canopy and ground surface, as well as the interactions between them, is explicitly considered in the model. More specifically, the leaf stomata control of water flow through plants is expressed as resistance terms r_{st} (Eqn S1-12) that aggregate the different r_{st_min} and r_{st_max} of shrubs and grasses (Table S1) and is upscaled to canopy resistance r_c (Eqn S1-11) by considering the aggregated LAI (Eqn S1-13) between shrubs and grasses.

The connectivity between plant and atmosphere was qualified by aerodynamic resistance which aggregated canopy height (r_{aV}, Eqn S1-9) between shrubs and grasses. The connectivity between soil and atmosphere expressed as aerodynamic resistance for ground surface (r_{aG}, Eqn S1-10) are accounted for ET partition. The connectivity between roots and different soil layers via root uptake was accounted for by transpiration partition between shrubs and grasses. The difference of the i^{th} soil layer water content ($\theta_{grass,i}$ and $\theta_{shrub,i}$) and fractions of water use of the i^{th} soil layer water by grasses and shrubs ($w_{grass,i}$ and $w_{shrub,i}$) were quantified by the stable isotope tracing approach (Method S2; Fig. S2) and aggregated corresponding to their roots connections (N_{grass} and N_{shrub}) (Eqns S1-16, S1-17) to represent the total plant water use (Eqn S1-15). The connectivity of water vapor through the soil layer is described by surface soil resistance r_{ss} (Eqn S1-18), which is parameterized by the aggregated volumetric soil water content of the first soil layer θ_1 (Eqn S1-19) between shrubs and grasses. Third, the model is solved by a Newton–Raphson scheme for the vegetation canopy T_L and ground temperature T_G separately, which is useful for partitioning the evapotranspiration components without radiometric temperature observations.

The model forcing includes constant parameters and the variable atmospheric forcing and seasonally variable plant and soil properties, such as vegetation coverage and soil water content. Specifically, the model was driven by fixed parameters (e.g. a clumping factor C_{LAI}, maximum and minimum stomata resistance r_{st_min} and r_{st_max}) and was driven by field observations of the following variables: (1) micrometeorological variables at hourly scale, including air temperature T_a, relative humidity of air h_a, downward shortwave radiation S_d, downward longwave radiation L_d, wind speed u, and air pressure P; (2) plant variables of each dominant species, including plant coverage f, leaf area index LAI, and canopy height Z_V; and (3) soil variables, including surface soil temperature T_{soil} at a depth Z_{soil} (m) and total available volumetric soil-water content θ. In this study, the root-mean-square difference (RMSD), the I index (Willmott, 1981; Cai *et al.*, 2015), and the coefficient of determination r^2 were used to evaluate model performance for the water and energy flux simulations.

Transpiration flux partitioning between shrubs and grass

A two-source mixing model has often been used to quantify source contributions (Phillips *et al.*, 2005; Ward *et al.*, 2011). We assumed that the total transpiration flux T was a mixture of grass transpiration T_{grass} and shrub transpiration T_{shrub} in the shrub-encroached grassland system:

$$T = CT_{shrub} + (1 - C)\,T_{grass} \quad \text{Eqn 1}$$

where C is the contribution of shrubs to the total transpiration flux.

Shrub encroachment upper and lower limits (with or without full shrub coverage) and the corresponding LAI, canopy height, and soil water content were established to estimate the upper and lower limits of transpiration. The two-source mixing model was used to calculate the transpiration fractions from shrubs (T_{shrub}/T) and from grasses (T_{grass}/T):

$$C = \frac{T - T_{grass}}{T_{shrub} - T_{grass}} \quad \text{Eqn 2}$$

Results

Model performance for determining evapotranspiration in a shrub-encroachment ecosystem

A very good agreement between measurements and simulations was found for net radiation R_n, latent heat flux lET, and soil heat flux G, with high I index (0.90–0.98) and small RMSD values (6.1–50.17 W m^{-2}) (Fig. 2; Table 1) during the growing season. The simulations of sensible heat flux H deviated from the 1 : 1 line with higher RMSD values (82.3 W m^{-2}), but this is not a serious concern in this study. The T_L and T_G values measured using a handheld infrared radiation thermometer were in good agreement with the model simulations, with r^2 values of 0.64 and 0.40 respectively.

Temporal variations of lET and *T*/ET

Both the sub-daily and day-to-day variations of lET were well simulated during the growing season (Fig. 3). The observed values measured by the Bowen ratio method (model simulated) of mean daily lET ranged from 6.8 W m^{-2} (−65.39 W m^{-2}) to 304.68 W m^{-2} (318.09 W m^{-2}), with average values of 153.79 ± 67.7% (149.3 ± 80.1%) from June to August. The lET showed wide sub-daily variations (from 09:00 to 16:00 h), with average values of 40.7 ± 22.68 W m^{-2} (62.9 ± 32 W m^{-2}). Both the sub-daily and day-to-day variations in *T*/ET were simulated from June to August (Fig. 4). The seasonal variations of *T*/ET ranged from 15% to 68.5%, with average values of 43.8 ± 14.2% from June to August.

Transpiration flux partitioning between shrubs and grasses

Both the sub-daily and day-to-day variations in transpiration flux were further partitioned between the shrubs and grasses based on the two-source mixing model (Fig. 5). The daily contribution of grasses (shrubs) to total transpiration ranged from 10.6% (21.6%) to 78.3% (89.44%), with mean values of 49.5 ± 15.1% (50.5 ± 15.1%) from June to August. The mean sub-daily variations for T_{grass}/T and T_{shrub}/T were 3.2 ± 2.9% (3.1 ± 3.0%) from June to August.

Seasonal variations in ET flux were further partitioned among shrub and grass transpiration and soil evaporation based on their contributions to total ET flux (Fig. 6). The seasonal mean contributions of the grass, shrub, and soil fractions to total ET flux were 24 ± 13%, 20 ± 4%, and 56 ± 16% respectively from June to August. The mean sub-daily variations of the contributions of

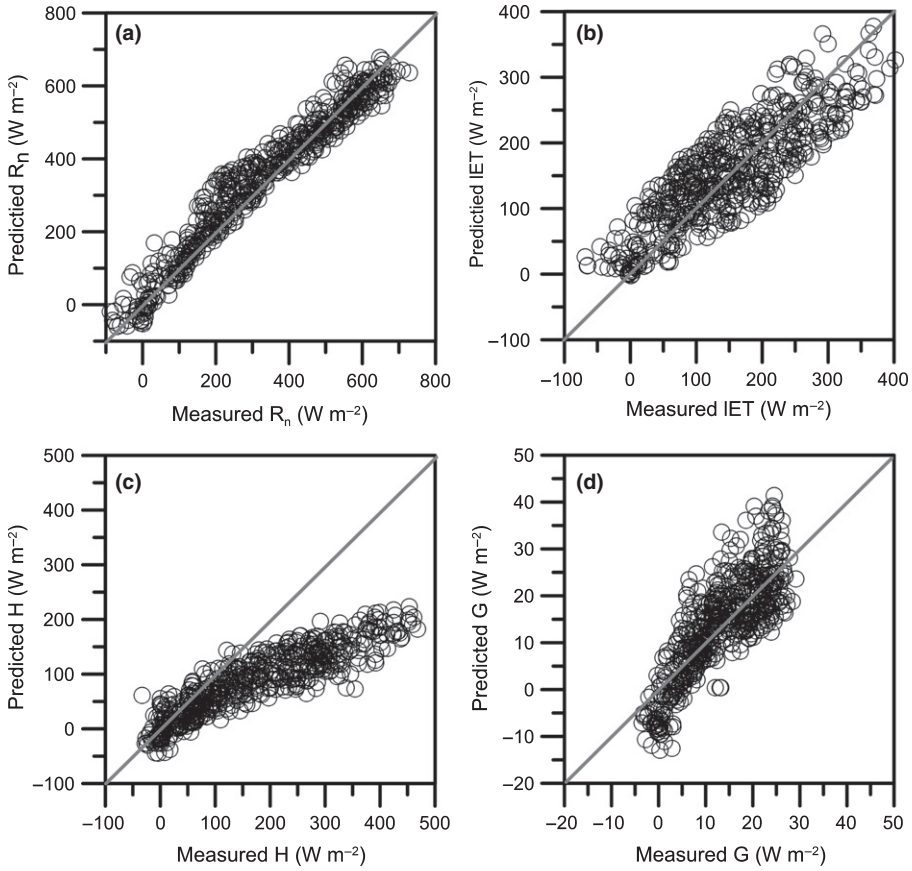

Fig. 2 Comparison of (a) net radiation R_n, (b) latent heat lET, (c) sensible heat flux H, and (d) ground heat flux G between measured and predicted values during the growing season. The statistics are summarized in Table 1.

Table 1 Statistics of model performance for energy flux and surface temperature in a shrub-encroached grassland ecosystem

Variable	R_n	lET	H	G	T_L	T_G
r^2	0.96	0.74	0.81	0.70	0.64	0.40
I index	0.98	0.95	0.81	0.90	N/A	N/A
RMSD (W m^{-2})	49.39	50.17	82.3	6.1	N/A	N/A
n	581	581	581	581	95	95

R_n, net radiation; lET, latent heat flux; H, sensible heat flux; G, ground heat flux; T_G, ground surface temperature; T_L, canopy leaf temperature; RMSD, root-mean-square difference.

the grass, shrub, and soil fractions to total ET flux were $1.5 \pm 1.1\%$, $1.5 \pm 1.1\%$, and $1.6 \pm 1.6\%$ respectively from June to August.

Sensitivity analysis

To account for the uncertainties and errors of the model, the sensitivity analysis for ET subcomponents was quantified for each input parameter and measurement variable. Table 2 summarizes the sensitivities of lET and *T*/ET to certain parameters and driving variables. Among those parameters, r_{st_min} was the most influential in changing lET; a 30% error in this parameter can introduce 8.4% error in lET on average. Shrub coverage f was the second most influential parameter in changing lET. Although this possible error range is not always negligible, it is not a serious issue. Moreover, the value of S_i for *T*/ET is generally small, suggesting that *T*/ET is insensitive to errors in the assigned values of all these parameters. h_a was the most influential variable in changing lET and can produce up to 7% error in lET if there is 5% error in h_a. Such an error range would be a minor problem in practice. As for *T*/ET, T_a and LAI were most influential, although 5% errors in these parameters introduced an error of only 1% in *T*/ET.

To account for model uncertainties and errors caused by individual inputs of shrubs or grasses, a sensitivity analysis of the input parameters and variables was quantified for shrubs and grasses (Table 3). The sensitivities of lET and *T*/ET to some parameters and driving variables were found to vary with shrub coverage f. As shrub coverage expanded, the sensitivities of lET and *T*/ET to certain shrub parameters (e.g. r_{st_min} and C_{LAI}) and driving variables (LAI, Z_V, and soil moisture) increased. The opposite situation was found for grasses at the study site; LAI_{grass} was the most influential variable in changing lET, followed by θ_{grass}. A 30% error in LAI_{grass} can introduce 11.4% error in lET on average. Moreover, the value of S_i for T/ET is generally small for both shrub and grass patches, suggesting that *T*/ET is insensitive to errors in the assigned values of all these parameters. Consequently, the estimated values of lET and *T*/ET are considered to be robust and acceptable, even if possible errors exist in the assigned model parameters and/or measured variables.

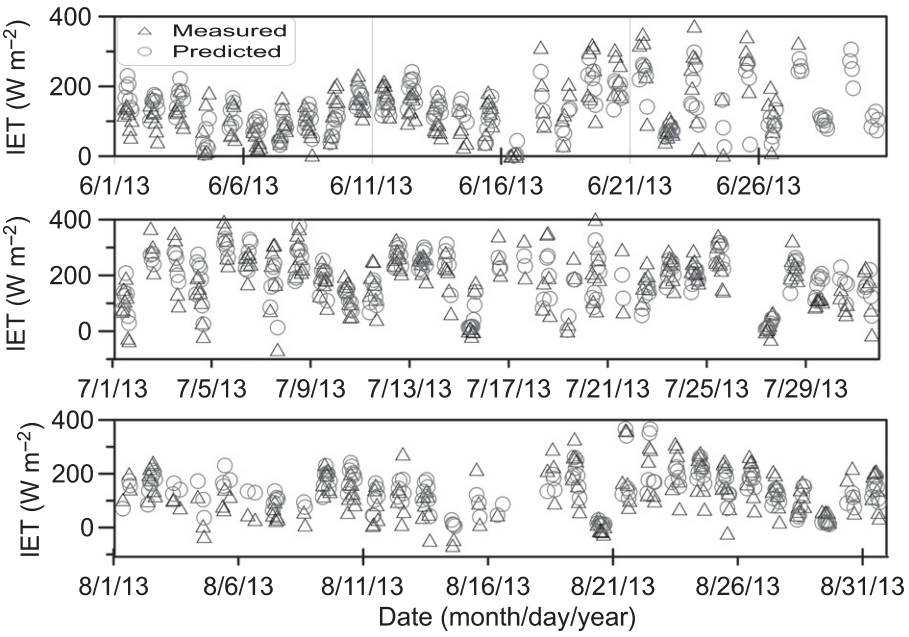

Fig. 3 Temporal variations of the predicted and measured hourly latent heat flux lET (l is the latent heat of vaporization and ET is the evapotranspiration) during the growing season.

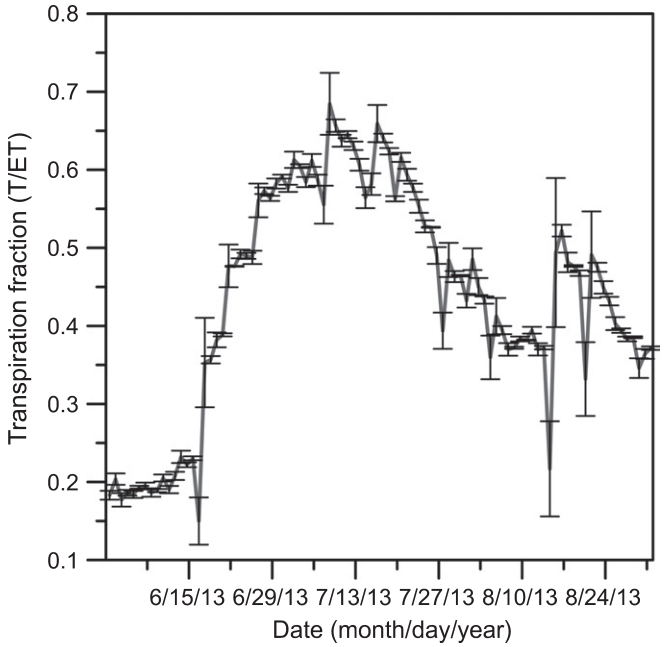

Fig. 4 Temporal variations in transpiration fraction *T*/ET. Error bar represents the daily standard deviation of *T*/ET from 09:00 to 16:00 h for each simulation day.

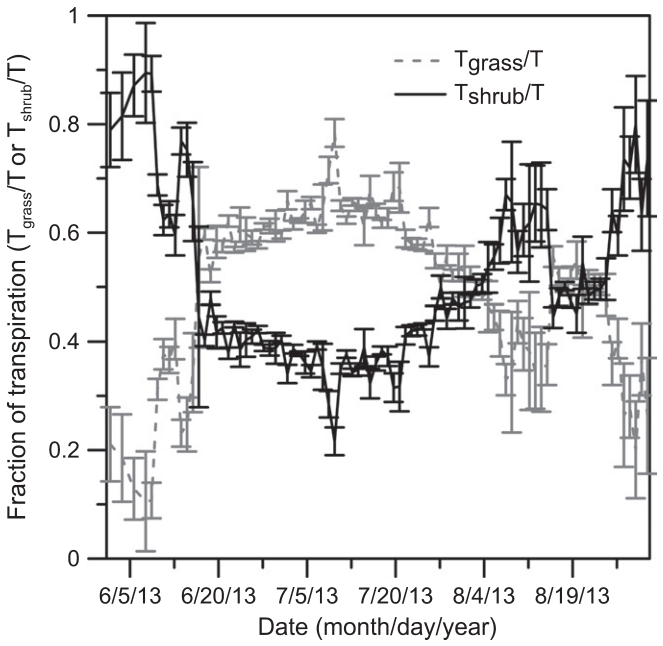

Fig. 5 Temporal variation in the shrub and grass transpiration fractions T_{shrub}/ET and T_{grass}/ET during the growing season. The error bar represents ± SD from 09:00 to 16:00 h for each simulation day.

Temporal variations of ET flux and *T*/ET under shrub-encroachment scenarios

The effects of shrub encroachment were quantified by changes of shrub coverage *f* and corresponding ecohydrological connectivity changes caused by shift of ecosystem structure (e.g. vegetation composition, LAI and Z_V) and total soil water use. Shrub encroachment effects on bare soil are highly site specific and show no change by meta-analyses (Eldridge *et al.*, 2015). Previous studies show that increasing precipitation from xeric to mesic ecosystems produces an associated increase in total vegetation cover, which results in reduced bare soil as a cover class (Schlesinger *et al.*, 1990; Huxman *et al.*, 2005). Considering that precipitation is almost constant in this area and the site was almost fully covered with vegetation during the observation period, a two-layer model (no bare soil) framework was used in this study. Therefore, shrub encroachment effects for bare soil were assumed to involve no changes in the model settings for shrub encroachment scenarios. Based on the calibrated model, a series of shrub encroachment scenarios with relative shrub coverage ranging

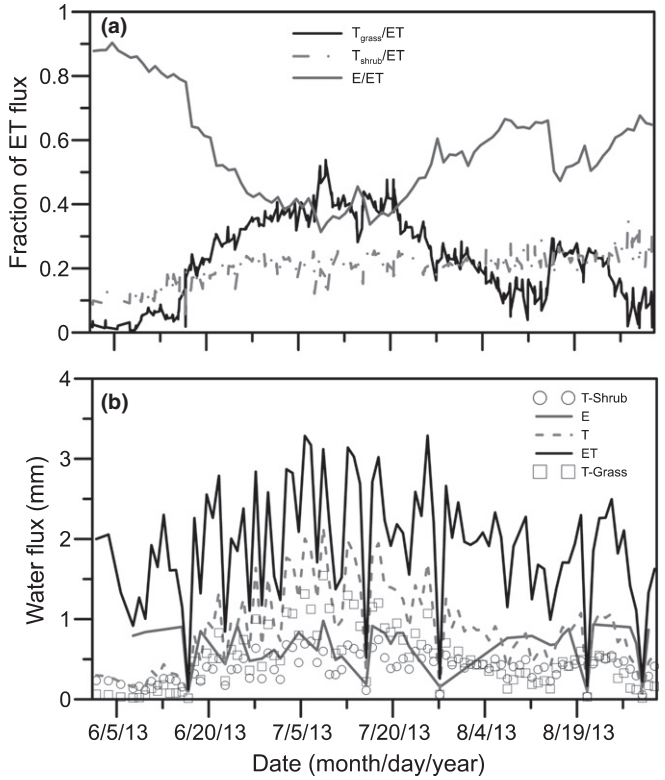

Fig. 6 Temporal variation of (a) the shrub and grass transpiration fractions T_{shrub}/ET and T_{grass}/ET and the soil evaporation faction E/ET and (b) water component flux of ET for each investigation day within the growing season.

Table 2 Mean and standard deviation (SD) of the sensitivity coefficients S_i of the evapotranspiration ET and transpiration fraction T/ET to the assigned model parameters and measured parameters

	Mean (SD)	
Model input	ET	T/ET
Parameters		
r_{st_min}	−0.28 (0.14)	−0.08 (0.02)
r_{st_max}	−0.01 (0.08)	0.00 (0.01)
α_V	−0.17 (0.23)	−0.02 (0.03)
α_G	−0.01 (0.06)	0.01 (0.01)
C_{LAI}	0.02 (0.01)	0.06 (0.03)
r_{ss}	−0.05 (0.02)	0.06 (0.02)
f	−0.22 (0.23)	0.02 (0.01)
Driving variables		
S_d	0.72 (0.31)	0.00 (0.20)
L_d	0.84 (0.58)	−0.03 (0.04)
u	0.08 (0.15)	0.00 (0.03)
T_a	0.74 (0.64)	0.21 (0.19)
h_a	−1.31 (1.02)	0.12 (0.22)
P	−0.04 (0.15)	−0.01 (0.03)
LAI	0.42 (0.26)	0.26 (0.25)
Z_v	0.23 (0.53)	0.03 (0.09)
T_{soil}	0.24 (0.14)	−0.17 (0.10)
θ	0.42 (0.43)	0.15 (0.12)

r_{st_min}, minimum stomata resistance; r_{st_max}, maximum stomata resistance; α_V, albedo of vegetation canopy; α_G, albedo of ground surface; C_{LAI}, clumping factor for canopy structure; r_{ss}, thermal conductivity of surface soil; f, shrub coverage; S_d, downward longwave radiation; L_d, downward longwave radiation; u, wind speed; T_a, air temperature; h_a, relative humidity; P, air pressure; LAI, leaf area index; Z_v, vegetation height; T_{soil}, soil surface temperature at depth Z_{soil}; θ, volumetric soil water content.

from 0% to 100% at intervals of 20% were evaluated, and the effects of shrub encroachment on processes governing terrestrial–atmospheric water fluxes were quantified. According to the degree of shrub encroachment, the factor weighting between shrub coverage f and grass coverage $1-f$ was changed in the model, as well as the corresponding model parameters, including minimum stomata resistance and clumping factor (Table S1), and variables such as leaf area index LAI, canopy height Z_V (Table S3) and ecosystem water availability θ (calculated as the weighted mean water availability between shrubs and grasses considering their water-use patterns (Method S2). The modeled results showed that shrub encroachment exerted greater influence on ET partitioning (e.g. T/ET) than that of total ET (Fig. 7). As shrub coverage f increased from 0% to 100%, the growing-season changes in mean ET ranged from 0.6% to 1.1% with seasonal variations ranging from 1.9% to 5.1%. The growing-season changes in mean T/ET ranged from −2.8% to −2.4%, with seasonal variations ranging from 1.8% to 4.8%.

Discussion

Flux partitioning in a shrub-encroached ecosystem

Using an updated multisource model together with *in situ* isotopic tracing and micrometeorological observations to investigate the effects of vegetation structure on land–atmosphere water exchanges revealed a reasonable agreement between the observed and modeled energy and water fluxes. Although previous studies used other methods to partition ET, there are several advantages of our coupled isotope and modeling approach. First, the model accounts for different plant types by weighting LAI, Z_V, and θ to represent the properties of the entire ecosystem, enabling the contribution of transpiration to be attributed between shrubs and grasses from an ecohydrological perspective (Method S1). In essence, it is a hybrid dual-source model (combining patches and layers) as reviewed by Zhang *et al.* (2016). In addition, the model presented here was not sensitive to possible uncertainties or errors in the assigned parameters and measured variables (Table 2). Second, differences of ecohydrological connectivity between shrubs and grasses were taken into consideration in the model (Fig. 1). In addition, the sensitivity of ET and T/ET to the model parameters assigned to shrubs and grasses under various scenarios can be quantified (Table 3). Although no statistically significant difference ($P > 0.05$) in soil moisture was found between grasses and shrubs in different layers (Table S2), there were some minor differences for the shallow layer and deep soil water (> 60 cm deep) due to the calcareous crust, which was also reported in previous studies (Li *et al.*, 2013). However, after considering the different water-use of shrubs and grasses as estimated by the isotopic approach (Methods S2), actual water use by shrubs and grasses was shown to be significantly different, particularly during dry seasons (soil water < 15% percentile; e.g. day of year (DOY)

Table 3 Mean and standard deviation (SD) of sensitivity coefficients S_i of evapotranspiration ET and transpiration fraction *T*/ET to the assigned model parameters by shrubs and grasses under four scenarios with shrub coverage of 15%, 25%, 31.4% and 43.47%

	Mean (SD)							
	ET				*T*/ET			
Model input	f_1	f_2	f_3	f_4	f_1	f_2	f_3	f_4
Shrubs								
r_{st_min}	−0.06 (0.03)	−0.10 (0.05)	−0.12 (0.06)	−0.16 (0.08)	−0.02 (0.00)	−0.03 (0.01)	−0.03 (0.01)	−0.04 (0.01)
C_{LAI}	0.00 (0.00)	0.00 (0.00)	0.01 (0.00)	0.01 (0.00)	0.01 (0.00)	0.01 (0.01)	0.02 (0.01)	0.02 (0.01)
LAI_{shrub}	0.04 (0.02)	0.04 (0.04)	0.04 (0.04)	0.08 (0.04)	0.01 (0.00)	0.01 (0.01)	0.01 (0.01)	0.02 (0.01)
$Z_{V\text{-}shrub}$	0.07 (0.00)	0.12 (0.00)	0.14 (0.00)	0.16 (0.00)	0.00 (0.00)	0.00 (0.00)	0.00 (0.00)	0.00 (0.00)
θ_{shrub}	0.08 (0.04)	0.13 (0.04)	0.13 (0.04)	0.17 (0.04)	0.01 (0.04)	0.02 (0.04)	0.02 (0.04)	0.03 (0.04)
Grasses								
r_{st_min}	−0.22 (0.11)	−0.18 (0.09)	−0.16 (0.08)	−0.12 (0.06)	−0.06 (0.02)	−0.05 (0.01)	−0.05 (0.01)	−0.04 (0.01)
C_{LAI}	0.02 (0.01)	0.02 (0.01)	0.01 (0.01)	0.01 (0.01)	0.05 (0.03)	0.05 (0.02)	0.04 (0.02)	0.04 (0.02)
LAI_{grass}	0.38 (0.02)	0.38 (0.04)	0.38 (0.04)	0.34 (0.04)	0.10 (0.00)	0.10 (0.01)	0.10 (0.01)	0.09 (0.01)
$Z_{V\text{-}grass}$	0.16 (0.00)	0.12 (0.00)	0.09 (0.00)	0.07 (0.00)	0.00 (0.00)	0.00 (0.00)	0.00 (0.00)	0.00 (0.00)
θ_{grass}	0.34 (0.04)	0.29 (0.04)	0.29 (0.04)	0.25 (0.04)	0.05 (0.04)	0.04 (0.04)	0.04 (0.04)	0.04 (0.04)

r_{st_min}, minimum stomata resistance of shrubs; C_{LAI}, clumping factor for shrub canopy structure; LAI_{shrub}, leaf area index of shrubs; $Z_{V\text{-}shrub}$, vegetation height of shrubs; θ_{shrub}, volumetric soil water content used by shrubs; r_{st_min}, minimum stomata resistance of grasses; C_{LAI}, clumping factor of canopy structure for grasses; LAI_{grass}, leaf area index of grasses; $Z_{V\text{-}grass}$, vegetation height of grasses; θ_{grass}, volumetric soil water content used by grasses.

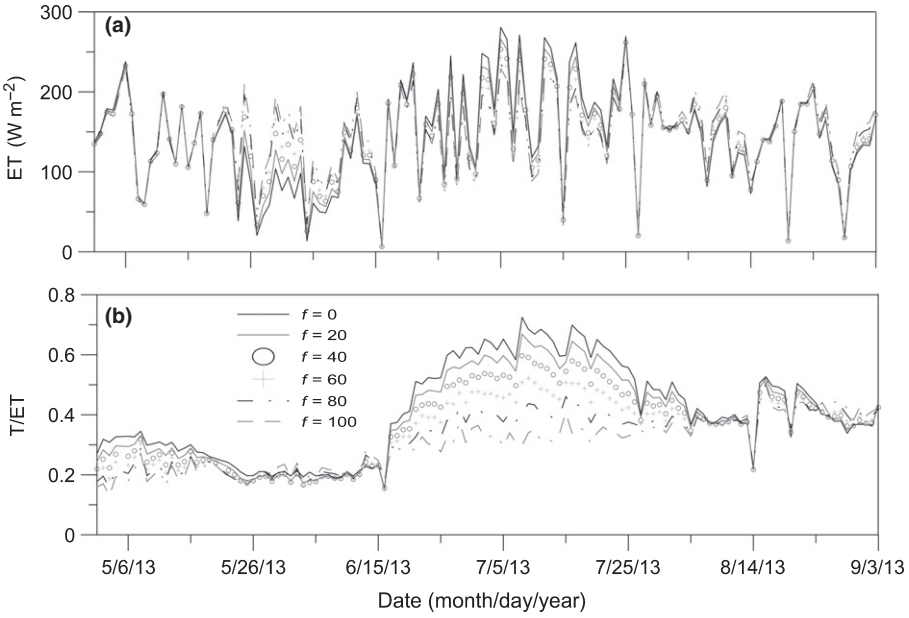

Fig. 7 Day-to-day variation of latent heat flux lET (l is the latent heat of vaporization and ET is evapotranspiration) and transpiration fraction *T*/ET under various shrub encroachment (*f* is shrub coverage) scenarios.

152–166). Because of root connections to deep soil water, shrubs can take up deep (up to 100 cm below the surface) soil water during dry seasons when shrubs dominate ecosystem transpiration (Fig. 5), which accounts for increasing ET flux and *T*/ET with greater shrub encroachment (Fig. 7). Third, aggregated stomatal control of transpiration at the canopy level r_c, coupling the differences in soil moisture, LAI, and Z_V, and the maximum and minimum stomatal resistance and the canopy structure between shrubs and grasses were explicitly considered in the model (Method S1; Table S1), whereas this was not the case in some previous two-source models. Previous studies highlighted LAI or soil moisture control for ecosystem *T*/ET (Hu *et al.*, 2009; Wang *et al.*, 2014; Wei *et al.*, 2017), However, canopy resistance r_c, which is a function of solar radiation, LAI, and soil water availability, was found to provide a better explanation of variations of *T*/ET than any single factor (e.g. LAI or θ) (Fig. S3). The results for r_c are quite comprehensive, aggregating the seasonal differences between shrubs and grasses with their distinct LAI and θ and their interactions with solar radiation. Among many single contributing factors (e.g. total LAI, total θ, and S_d), the highest r^2 value (0.82) was found between total LAI and *T*/ET, followed by θ with $r^2 = 0.48$ in this study. Therefore, leaf development (changes in LAI) and trade-off between shrubs and grasses dominated the seasonality of *T*/ET in the study site. Model-based analyses indicated that consideration of the different ecohydrological connectivities between shrubs and grasses (e.g. root

connections, canopy resistance) was important for illustrating the effects of shrub encroachment on ET and its components (Figs 7, 8). However, the model still requires modification and improvement. For example, the differences in microclimatic factors (e.g. wind speed) between shrubs and grasses were not fully considered in this model, and the isotopic-based water uptake may have resulted in errors (e.g. in upper and lower limits), which would produce errors in the ET subcomponent simulations. In addition, different to previous modeling framework (Yu & D'Odorico, 2014), the contribution of grass beneath shrubs was not considered independently but incorporated with grasses as a whole while assuming a similar water-use pattern. Also,

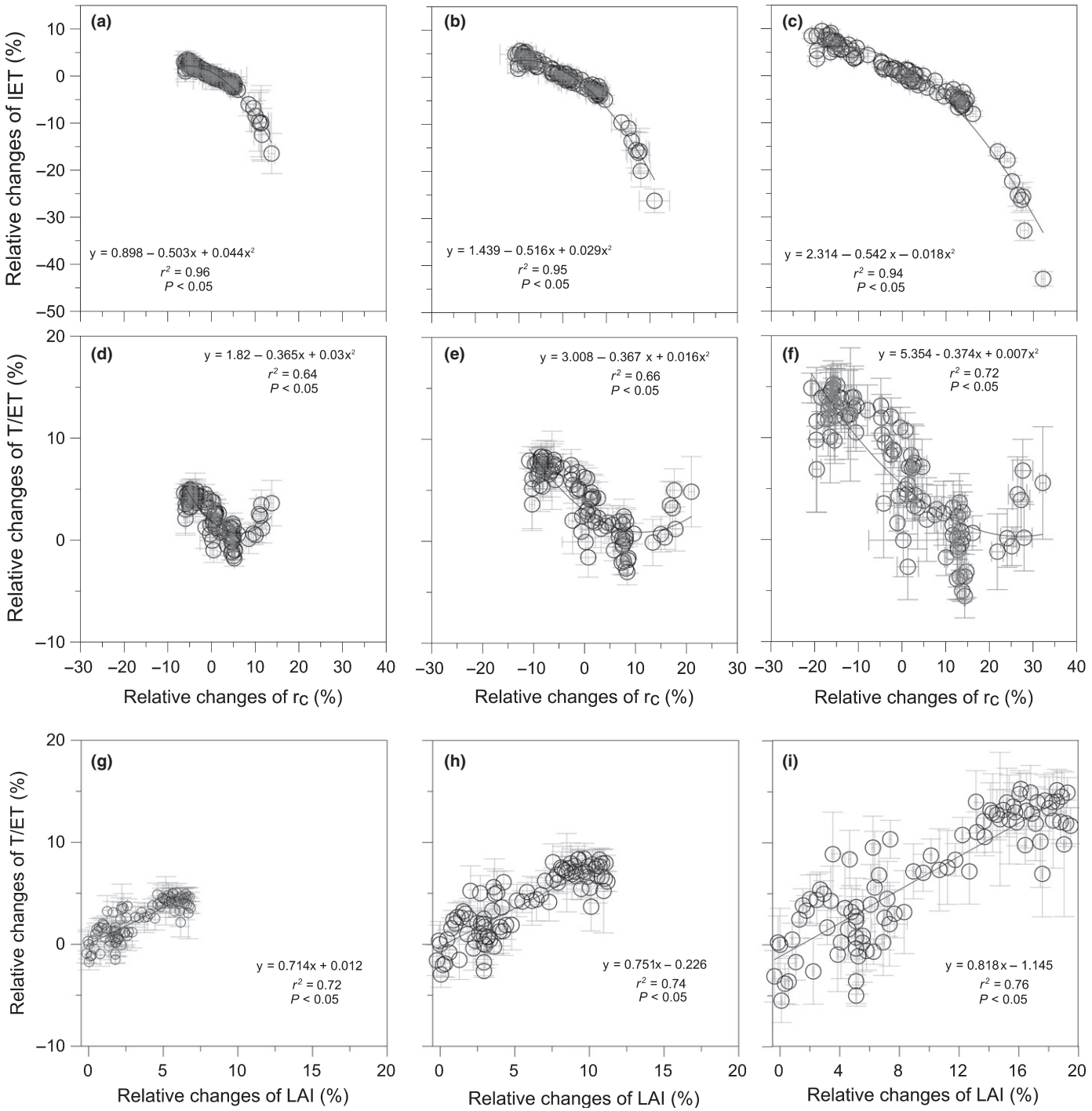

Fig. 8 Relationship between relative changes (compared with actual shrub coverage of 15%) in canopy resistance r_c and latent heat flux lET under three shrub-encroachment scenarios with shrub coverage of (a) 25%, (b) 31.4%, and (c) 43.5%, and transpiration fraction *T*/ET with shrub coverage of (d) 25%, (e) 31.4%, and (f) 43.5%. Relationship between relative changes in leaf area index LAI with *T*/ET with shrub coverage of (g) 25%, (h) 31.4%, and (i) 43.5% during the growing season.

evaporation of rainfall intercepted by the vegetation canopy was not considered in the model, which may have introduced a potential bias into the results. Previous experimental results at this site quantified the relationship between interception amount for shrubs (grasses) and rainfall amount (Peng *et al.*, 2014). As summarized in Table 4, the estimated total interception amount accounted for 9.6% of total precipitation amount. During the day, the estimated interception amount accounted for 5.6% (10.1%) of total ET (T). To qualify the uncertainties caused by interception, ET partition results (T/ET, T_{grass}/T and T_{shrub}/T) were compared between datasets for rain/all days ($n = 46/92$) and sunny days ($n = 46$). Statistical results indicated no significant difference ($P > 0.05$) in ET partition results between the datasets for rain (all) days and sunny days. The errors caused by intercepted rainfall accounted for < 2% (3%) of T/ET (T_{grass}/T and T_{shrub}/T). Therefore, although possible errors may exist in the model, the ET partition results are quite robust and reasonable.

Table 4 Statistical data for precipitation, evapotranspiration ET, and their components under rainy and rain-free days during the growing season

Items	Total
Precipitation amount (mm)	182.6
Day (night)-time rain amount (mm)[a]	102.1 (80.5)
Interception amount (mm)[b]	17.7
Interception amount for shrubs (grasses)[c] (mm)	7.3 (10.4)
Day (night)-time rain amount (mm)[a]	102.1 (107.3)
Rainy (rain-free) days	46 (46)
Daytime ET (mm)[a]	174.6
Daytime T (E) (mm)[a]	81.7 (93.27)
T/ET (mean ± SD) ($n = 92$)	0.44 ± 0.15
Sunny days T/ET (mean ± SD) ($n = 46$)[d]	0.42 ± 0.14
Rain days T/ET (mean ± SD) ($n = 46$)[d]	0.45 ± 0.15
T_{grass}/T (mean ± SD) ($n = 92$)	0.49 ± 0.15
Sunny days T_{grass}/T (mean ± SD) ($n = 46$)[e]	0.48 ± 0.15
Rain days T_{grass}/T (mean ± SD) ($n = 46$)[e]	0.51 ± 0.15
T_{shrub}/T (mean ± SD) ($n = 92$)	0.50 ± 0.15
Sunny days T_{shrub}/T (mean ± SD) ($n = 46$)[f]	0.51 ± 0.15
Rain days T_{grass}/T (mean ± SD) ($n = 46$)[f]	0.49 ± 0.15

[a]Day-time (09:00–18:00 h) and night-time 18:00–8:00 h China Standard Time.
[b]Estimated by previous experimental results.
[c]Estimated by previous experimental results.
[d]Not significantly different at the 5% level for transpiration fraction T/ET between the rain-days dataset ($n = 46$) and the dataset with no rainy days ($n = 46$).
[e]Not significantly different at the 5% level for fraction of grasses for total transpiration T_{grass}/T between the rain days dataset and the dataset with no rainy days.
[f]Not significantly different at the 5% level for the fraction of shrubs over total transpiration T_{shrubs}/T between the rain days dataset and the dataset with no rainy days.

Effects of shrub encroachment on ET partitioning and climatic implications

Shrub encroachment alters the canopy structure and biophysical processes, with one of the main changes being an increase in shrub cover and a decrease in grass cover (Eldridge *et al.*, 2015). This will then result in changes in canopy LAI, Z_V, and rooting depth, which are key variables for ecohydrological processes such as rainfall redistribution, infiltration, runoff generation, and ET or its components (Huxman *et al.*, 2005; Li *et al.*, 2013). Overall, this simulation indicated that shrub-encroachment processes resulted in larger changes in ET components than in ET flux and that shrub encroachment effects on ET flux and T/ET varied seasonally depending on ecosystem aridity and plant dynamics. Based on soil water content during the growing season and using < 15% or > 85% percentiles of soil water content to define dry or wet periods, investigations showed that shrub water uptake from deep soil layers is vital for sustaining ecosystem transpiration in dry periods. Hence, shrubs have the advantage of increasing T/ET under low-rainfall conditions. Shrub encroachment has increased ecosystem water availability, leading to obvious increases in ET flux and T/ET during dry periods (e.g. DOY 152–166) (Fig. 7). This study is consistent with previous studies which showed that shrubs can take up water from deep soil and increases T/ET (Walter, 1971; Breshears & Barnes, 1999; House *et al.*, 2003; Budny & Benscoter, 2016). With increasing shrub coverage, total ecosystem LAI was decreased (Table S3), which increased the solar radiation reaching the ground surface and led

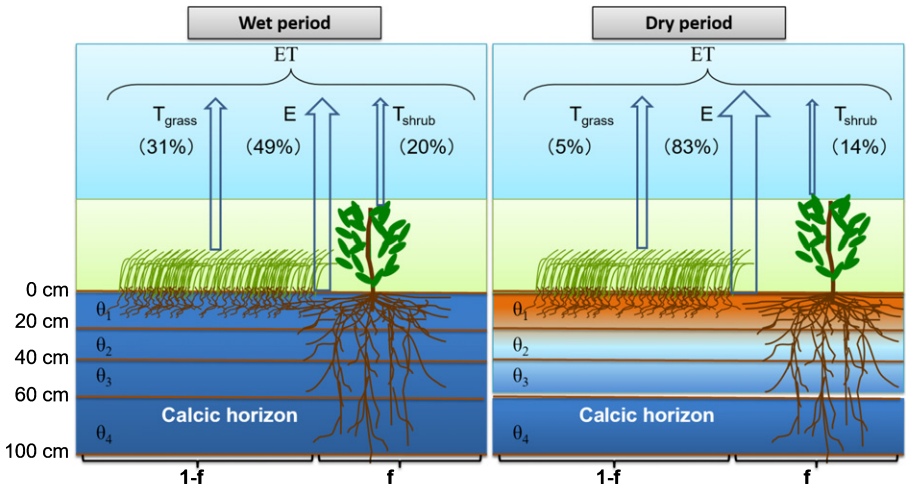

Fig. 9 Frameworks of ecohydrological connectivity scenarios of shrubs with coverage f and grasses under wet and dry seasons for evapotranspiration ET partitioning into soil evaporation E, grass transpiration T_{grass}, and shrub transpiration T_{shrub}. During the 'wet period', grasses can quickly use rapidly recharged surface soil water, whereas shrubs use soil water in proportion to the distribution of their roots at all depths for transpiration. During the 'dry season', shrubs can use deep soil water and dominate ecosystem transpiration.

to an increase in *E*. The situation at this site was different from previous studies (Schlesinger *et al.*, 1990; Martens *et al.*, 2000; Thompson *et al.*, 2017), which dealt with shrub invasion due to increasing precipitation increasing the vegetation cover and reducing the amount of solar radiation reaching the ground, subsequently reducing *E*, but agreed with the conclusion of Huxman *et al.* (2005). Those contrary effects of shrub encroachment on ET components related to the shrubs traits (Eldridge *et al.*, 2015) and varied across a climatic gradient (Huxman *et al.*, 2005). By comparing the current simulation results (shrub coverage, $f = 15\%$) with results from an earlier field investigation of shrub encroachment in this region with $f = 25\%$, 31.4% and 43.5% (Peng *et al.*, 2013), the effects of shrub encroachment on ET and *T*/ET were found to be well explained and quantified by changes in r_c, which integrated changes in soil water and ecosystem structure (e.g. LAI, Z_V and vegetation composition) caused by shrub-encroachment processes (Fig. 8). The effects of shrub encroachment on ET have a significant nonlinear negative relationship with changes in r_c caused by shrub-encroachment processes (Fig. 8a–c). The effects of shrub encroachment on aggregate *T*/ET were complex and were determined by the trade-off between the impacts of shrubs and grasses on seasonal variations of soil water and LAI (Fig. 8d–f). It is the traits of encroaching woody plants that determine the functional outcome of encroachment. Shrub encroachment results in increasing *T*/ET during dry periods, with a decrease in r_c by enhanced water uptake from the deep soil layer. Shrub encroachment decreases *T*/ET accompanied by an increase in r_c during the period of fast growth because of LAI decrease. The shrub encroachment effects on *T*/ET were dominated by shrubs when they increased their total water use during dry periods, but shifted to control by grasses when they increased their total LAI during the growing season (Fig. 7). Unlike the positive feedback of shrub encroachment (increase in total water use) on *T*/ET, negative feedback (decrease in total LAI) on *T*/ET was dominant during the growing season at the study site (Fig. 8g–i). This study therefore emphasizes the divergent ET partition responses between shrubs and grasses caused by the ecohydrological properties of each functional type.

A review by Huxman *et al.* (2005) confirmed that woody plant encroachment will alter *T*/ET and is largely driven by climate because more water will be recharged to the deep soil and *E* decreases as precipitation increases. Based on the analysis in this study, the adaptation of grasses and shrubs has been summarized with regard to their water use and transpiration strategies. On rainy days, grasses were found to respond quickly by taking up the shallow soil water that is rapidly recharged on days with rainfall. Grasses can achieve this because they have less stomata resistance and stronger transpiration than shrubs. Indeed, recent studies showed that the more efficient water usage by grasses was associated with high growth rate, which led to the species composition shift from shrubs to grasses in wet environments (Yu *et al.*, 2017) and the ecosystem transition from a shrub-dominated state to a grass-dominated state (Chen *et al.*, 2018). Shrubs, however, have a conservative strategy and can use deep soil water, which is useful during dry periods (Figs 5, 9). Therefore, with climate change, shrubs have a competitive advantage under a dry climate, whereas grass has a competitive advantage under wetter conditions. Our modeling results showed that shrub encroachment had relatively little influence on ET but did have an influence on the proportions of the components of ET (e.g. *T*/ET), which represents the relative contribution of ecological processes to the hydrological flux. This indicates that, with the spatial heterogeneity of vegetation, the different ecohydrological connectivities between soil water and different types of plants are important for accurate estimation of ET flux and its components.

Acknowledgements

The study was financially supported by the National Natural Science Foundation of China (41730854, 91425301, and 41671019) and the State Key Laboratory of Earth Surface Processes and Resource Ecology. L.W. acknowledges partial support from the Division of Earth Sciences of National Science Foundation (NSF EAR-1554894) and from the Agriculture and Food Research Initiative program (2017-67013-26191) of the USDA National Institute of Food and Agriculture.

Author contributions

P.W. and X-Y.L. designed the research. P.W. performed modeling simulation and sensitivity analysis. P.W., X-Y.L, L.W. and X.W. contributed to the interpretation and writing. P.W., X.H., Y.F. and Y.T. contributed to the field investigations. P.W. performed isotopic measurements and analysis.

ORCID

Lixin Wang http://orcid.org/0000-0002-8647-253X

References

Anderson MC, Norman JM, Mecikalski JR, Torn RD, Kustas WP, Basara JB. 2004. A multiscale remote sensing model for disaggregating regional fluxes to micrometeorological scales. *Journal of Hydrometeorology* **5**: 343–363.

Archer SR. 2010. Rangeland conservation and shrub encroachment: new perspectives on an old problem. In: du Toit JT, Kock R, Deutsch JC, eds. *Wild rangelands: conserving wildlife while maintaining livestock in semi-arid ecosystems.* Chichester, UK: John Wiley & Sons, 53–97.

Archer S, Schimel DS, Holland EA. 1995. Mechanisms of shrubland expansion: land use, climate or CO_2? *Climate Change* **29**: 91–99.

Breshears DD, Barnes FJ. 1999. Interrelationships between plant functional types and soil moisture heterogeneity for semiarid landscapes within the grassland/forest continuum: a unified conceptual model. *Landscape Ecology* **14**: 465–478.

Brooks PD, Chorover J, Fan Y, Godsey SE, Maxwell RM, McNamara JP, Tague C. 2015. Hydrological partitioning in the critical zone: recent advances and opportunities for developing transferable understanding of water cycle dynamics. *Water Resources Research* **51**: 6973–6987.

Budny ML, Benscoter BW. 2016. Shrub encroachment increases transpiration water loss from a subtropical wetland. *Wetlands* **36**: 631–638.

Cai MY, Wang L, Parkes SD, Strauss J, McCabe MF, Evans JP, Griffiths AD. 2015. Stable water isotope and surface heat flux simulation using ISOLSM: evaluation against *in-situ* measurements. *Journal of Hydrology* **523**: 67–78.

Chen N, Jayaprakash C, Yu K, Guttal V. 2018. Rising variability, not slowing down, as a leading indicator of a stochastically driven abrupt transition in a dryland ecosystem. *American Naturalist* **191**: 1–14.

Coetzee BWT, Tincani L, Wodu Z, Mwasi SM. 2008. Overgrazing and bush encroachment by *Tarchonanthus camphoratus* in a semi-arid savanna. *African Journal of Ecology* **46**: 449–451.

D'Odorico P, He Y, Collins S, De Wekker SF, Engel V, Fuentes JD. 2013. Vegetation–microclimate feedbacks in woodland–grassland ecotones. *Global Ecology and Biogeography* **22**: 364–379.

D'Odorico P, Okin GS, Bestelmeyer BT. 2011. A synthetic review of feedbacks and drivers of shrub encroachment in arid grasslands. *Ecohydrology* **5**: 520–530.

Eldridge DJ, Bowker MA, Maestre FT, Roger E, Reynolds JF, Whitford WG. 2011. Impacts of shrub encroachment on ecosystem structure and functioning: towards a global synthesis. *Ecology Letters* **14**: 709–722.

Eldridge DJ, Wang L, Ruiz-Colmenero M. 2015. Shrub encroachment alters the spatial patterns of infiltration. *Ecohydrology* **8**: 83–93.

Fisher JB, Melton F, Middleton E, Hain C, Anderson M, Allen R. 2017. The future of evapotranspiration: global requirements for ecosystem functioning, carbon and climate feedbacks, agricultural management, and water resources. *Water Resources Research* **53**: 2618–2626.

Good SP, Noone D, Bowen G. 2015. Hydrologic connectivity constrains partitioning of global terrestrial water fluxes. *Science* **349**: 175.

Guan HD, Wilson JL. 2009. A hybrid dual-source model for potential evaporation and transpiration partitioning. *Journal of Hydrology* **377**: 405–416.

He Y, D'Odorico P, Wekker SFJD, Fuentes JD, Litvak M. 2010. On the impact of shrub encroachment on microclimate conditions in the northern Chihuahuan desert. *Journal of Geophysical Research: Atmospheres* **115**: 6128.

House JI, Archer S, Breshears DD, Scholes RJ. 2003. Conundrums in mixed woody–herbaceous plant systems. *Journal of Biogeography* **30**: 1763–1777.

Hu ZM, Yu GR, Zhou YL, Sun XM, Li YL, Shi PL, Wang YF, Song X, Zheng Z, Zhang L *et al.* 2009. Partitioning of evapotranspiration and its controls in four grassland ecosystems: application of a two-source model. *Agriculture and Forest Meteorology* **149**: 1410–1420.

Huxman TE, Wilcox BP, Breshears DD, Scott RL, Snyder KA, Small EE. 2005. Ecohydrological implications of woody plant encroachment. *Ecology* **86**: 308–319.

Jasechko S, Sharp ZD, Gibson JJ, Birks SJ, Yi Y, Fawcett PJ. 2013. Terrestrial water fluxes dominated by transpiration. *Nature* **496**: 347.

Jones H. 1992. *Plants and microclimate*. New York, NY, USA: Cambridge University Press.

Katul GG, Oren R, Manzoni S, Higgins C, Parlange MB. 2012. Evapotranspiration: a process driving mass transport and energy exchange in the soil–plant–atmosphere–climate system. *Reviews of Geophysics* **50**: 1209–8755.

Kendall C, McDonnell JJ. 1998. *Isotope tracers in catchment hydrology*. Amsterdam, Netherlands: Elsevier.

Kool D, Agam N, Lazarovitch N, Heitman JL, Sauer TJ, Ben GA. 2014. A review of approaches for evapotranspiration partitioning. *Agriculture and Forest Meteorology* **184**: 56–70.

Li S, Kang SZ, Zhang L, Li FS, Zhu ZL, Zhang BZ. 2008. A comparison of three methods for determining vineyard evapotranspiration in the arid desert regions of northwest China. *Hydrological Processes* **22**: 4554–4564.

Li XY, Zhang SY, Peng HY, Hu X, Ma YJ. 2013. Soil water and temperature dynamics in shrub-encroached grasslands and climatic implications: results from Inner Mongolia steppe ecosystem of north China. *Agriculture and Forest Meteorology* **171–172**: 20–30.

Martens SN, Breshears DD, Meyer CW. 2000. Spatial distributions of understory light along the grassland/forest continuum: effects of cover, height, and spatial pattern of tree canopies. *Ecological Modelling* **126**: 79–93.

Maxwell RM, Condon LE. 2016. Connections between groundwater flow and transpiration partitioning. *Science* **353**: 377.

Miller GR, Cable JM, Mcdonald AK, Bond B, Franz TE, Wang L. 2012. Understanding ecohydrological connectivity in savannas: a system dynamics modelling approach. *Ecohydrology* **5**: 200–220.

Moran MS, Scott RL, Keefer TO, Emmerich WE, Hernandez M, Nearing GS. 2009. Partitioning evapotranspiration in semiarid grassland and shrubland ecosystems using time series of soil surface temperature. *Agriculture and Forest Meteorology* **149**: 59–72.

Neilson RP. 1986. High-resolution climatic analysis and southwest biogeography. *Science* **232**: 27–34.

Norman JM, Anderson MC, Kustas WP, French AN, Mecikalski J, Torn R, Diak GR, Schmugge TJ, Tanner BCW. 2003. Remote sensing of surface energy fluxes at 10^1-m pixel resolutions. *Water Resources Research* **39**: 1221.

Norman JM, Becker F. 1995. Terminology in thermal infrared remote sensing of natural surfaces. *Agriculture and Forest Meteorology* **77**: 153–166.

Peng HY, Li XY, Li GY, Zhang ZH, Zhang SY, Li L, Zhao GQ, Jiang ZY, Ma YJ. 2013. Shrub encroachment with increasing anthropogenic disturbance in the semiarid Inner Mongolian grasslands of China. *Catena* **109**: 39–48.

Peng HY, Li XY, Tong SY. 2014. Effects of shrub (*Caragana microphylla* Lam.) encroachment water redistribution and utilization in typical steppe of Inner Mongolian. *Acta Ecologica Sinica* **34**: 2256–2265 (in Chinese).

Phillips DL, Newsome SD, Gregg JW. 2005. Combining sources in stable isotope mixing models: alternative methods. *Oecologia* **144**: 520–527.

Schlesinger WH, Reynolds JF, Cunningham GL, Huenneke LF, Jarrell WM, Virginia RA, Whitford WG. 1990. Biological feedbacks in global desertification. *Science* **247**: 1043–1048.

Scott RL, Huxman TE, Cable WL, Emmerich WE. 2006a. Partitioning of evapotranspiration and its relation to carbon dioxide exchange in a Chihuahuan Desert shrubland. *Hydrological Processes* **20**: 3227–3243.

Scott RL, Huxman TE, Williams DG, Goodrich DC. 2006b. Ecohydrological impacts of woody-plant encroachment: seasonal patterns of water and carbon dioxide exchange within a semiarid riparian environment. *Global Change Biology* **12**: 311–324.

Shuttleworth WJ, Wallace J. 1985. Evaporation from sparse crops – an energy combination theory. *Quarterly Journal of the Royal Meteorological Society* **111**: 839–855.

Sprenger M, Leistert H, Gimbel K, Weiler M. 2016. Illuminating hydrological processes at the soil–vegetation–atmosphere interface with water stable isotopes. *Reviews of Geophysics* **54**: 674–704.

Thompson JA, Zinnert JC, Young DR. 2017. Immediate effects of microclimate modification enhance native shrub encroachment. *Ecosphere* **8**: e01687.

Van Auken OW. 2000. Shrub invasions of North American semiarid grasslands. *Annual Review of Ecology and Systematics* **31**: 197–215.

Van Auken OW. 2009. Causes and consequences of woody plant encroachment into western North American grasslands. *Journal of Environmental Management* **90**: 2931–2942.

Walter H. 1971. *Ecology of tropical and subtropical vegetation*. Edinburgh, UK: Oliver & Boyd.

Wang L, Caylor KK, Villegas JC, Barron-Gafford GA, Breshears DD, Huxman TE. 2010. Partitioning evapotranspiration across gradients of woody plant cover: assessment of a stable isotope technique. *Geophysical Research Letters* **37**: L09401.

Wang L, D'Odorico P. 2008. The limits of water pumps. *Science* **321**: 36–37.

Wang L, Good SP, Caylor KK. 2014. Global synthesis of vegetation control on evapotranspiration partitioning. *Geophysical Research Letters* **41**: 6753–6757.

Wang P, Li XY, Huang Y, Liu S, Xu Z, Wu X, Ma YJ. 2016. Numerical modeling the isotopic composition of evapotranspiration in an arid artificial oasis cropland ecosystem with high-frequency water vapor isotope measurement. *Agriculture and Forest Meteorology* **230–231**: 79–88.

Wang P, Yamanaka T. 2014. Application of a two-source model for partitioning evapotranspiration and assessing its controls in temperate grasslands in central Japan. *Ecohydrology* **7**: 345–353.

Wang P, Yamanaka T, Li XY, Wei ZW. 2015. Partitioning evapotranspiration in a temperate grassland ecosystem: numerical modeling with isotopic tracers. *Agriculture and Forest Meteorology* **208**: 16–31.

Wang L, Zou C, O'Donnell F, Good S, Franz S, Miller G, Caylor K, Cable J, Bond B. 2012. Characterizing ecohydrological and biogeochemical connectivity across multiple scales: a new conceptual framework. *Ecohydrology* **5**: 221–233.

Ward EJ, Semmens BX, Phillips DL, Moore JW, Bouwes N. 2011. A quantitative approach to combine sources in stable isotope mixing models. *Ecosphere* **2**: 195–201.

Wei Z, Yoshimura K, Wang L, Miralles D, Jasechko S, Lee X. 2017. Revisiting the contribution of transpiration to global terrestrial evapotranspiration. *Geophysical Research Letters* **44**: 2792–2801.

West AG, Patrickson SJ, Ehleringer JR. 2006. Water extraction times for plant and soil materials used in stale isotope analysis. *Rapid Communications in Mass Spectrometry* **20**: 1317–1321.

Whitley R, Beringer J, Hutley LB, Abramowitz G, Kauwe MGD, Evans B. 2016. Challenges and opportunities in modelling savanna ecosystems. *Biogeosciences Discussions* **14**: 4711–4732.

Williams DG, Cable W, Hultine K, Hoedjes JCB, Yepez EA, Simonneaux V, Er-Raki S, Boulet G, de Bruin HAR, Chehbouni A *et al.* 2004. Evapotranspiration components determined by stable isotope, sap flow and eddy covariance techniques. *Agricultural and Forest Meteorology* **125**: 241–258.

Willmott CJ. 1981. On the validation of models. *Physical Geography* **2**: 184–194.

Wu X, Liu H, Li X, Ciais P, Babst F, Guo W, Zhang C, Magliulo V, Pavelka M, Liu S *et al.* 2017. Differentiating drought legacy effects on vegetation growth over the temperate northern hemisphere. *Global Change Biology* **24**: 1–13.

Yu K, D'Odorico P. 2014. An ecohydrological framework for grass displacement by woody plants in savannas. *Journal of Geophysical Research: Biogeosciences* **119**: 192–206.

Yu K, Saha MV, D'Odorico P. 2017. The effects of interannual rainfall variability on tree–grass composition along Kalahari rainfall gradient. *Ecosystems* **20**: 975–988.

Zhang K, Kimball JS, Running SW. 2016. A review of remote sensing based actual evapotranspiration estimation: a review of remote sensing evapotranspiration. *WIREs Water* **3**: 834–853.

Zhang ZH, Li XY, Jiang ZY, Peng HY, Li L, Zhao GQ. 2013. Changes in some soil properties induced by re-conversion of cropland into grassland in the semiarid steppe zone of Inner Mongolia, China. *Plant and Soil* **373**: 89–106.

Zhang Z, Wang SP, Nyren P, Jiang GM. 2006. Morphological and reproductive response of *Caragana microphylla* to different stocking rates. *Journal of Arid Environments* **67**: 671–677.

Zhao L, Wang L, Cernusak LA, Liu X, Xiao H, Zhou M, Zhang S. 2016. Significant difference in hydrogen isotope composition between xylem and tissue water in *Populus euphratica*. *Plant, Cell & Environment* **39**: 1848–1857.

Supporting Information

Additional supporting information may be found online in the Supporting Information section at the end of the article:

Fig. S1 Schematic illustration of the two source model, redrawn from Wang & Yamanaka (2014).

Fig. S2 Water isotopes plot ($\delta^{18}O$ and $\delta^{2}H$) of soil water from different layers, xylem and leaf water of shrubs and grasses.

Fig. S3 Relationship between canopy resistance (r_c) and transpiration fraction (T/ET) for all hourly data sets during the growing season.

Table S1 Parameterization details of constant parameters in the model

Table S2 Summary of measured soil water by oven-dry method and representation of actual soil water uptake under shrubs and grasses under each observation day

Table S3 Summary of field investigation of vegetation property of shrub encroached grassland during growing season

Table S4 List of symbols in the modelling framework

Methods S1 Detailed description of the multi-source energy balance model.

Methods S2 Detailed description of water use pattern of shrub and grass by isotope tracing.

Please note: Wiley Blackwell are not responsible for the content or functionality of any Supporting Information supplied by the authors. Any queries (other than missing material) should be directed to the *New Phytologist* Central Office.